Kathmandu University
Journal of Science, Engineering and Technology

Rudraiah & Shashikala, Vol. 12, No. I, June, 2016, pp 1-12.

ORIGINAL RESEARCH ARTICLE OPEN ACCESS

EFFECTS OF PERMEABILITY AND ELECTRIC FIELD ON NONLINEAR OBERBECK ELECTRO-CONVECTION IN A VERTICAL POORLY CONDUCTING FLUID SATURATED POROUS CHANNEL

[1]Rudraiah N.*, [2]Shashikala B. S.
[1]National Research Institute for Applied Mathematics (NRIAM), #492/G, 7th Cross, 7th Block (West), Jayanagar, Bangalore -560082
[2]Department of Mathematics, Govt.S.K.S.J.T.I, K.R.Circle, Bangalore-01

*Corresponding author's e-mail: shashikala.somu@gmail.com
Received 23 May, 2015; Revised 14 March, 2016

ABSTRACT

The effects of permeability on nonlinear Oberbeck Electro-convection in a poorly conducting fluid saturated porous medium in a vertical channel, when the walls are held at different temperatures with temperature difference perpendicular to gravity, is studied using the modified Navier stokes equation in the presence of both induced and an applied electric field. Both analytical and numerical solutions for the non-linear coupled equations governing the motion are obtained and found that analytical solutions agree well with numerical solutions for values of the buoyancy parameter N <1. It is shown that OBEC can be controlled by maintaining the temperature difference either in the same direction or opposing the potential difference with a suitable value of electric number W. The effect of W on velocity, temperature, rate of heat transfer, skin friction and mass flow rate are computed and the results are depicted graphically. We found that the analytical solutions for velocity and temperature distributions are in close agreement with those obtained from the numerical method for small values of N. We also found that an increase in W accelerates the flow and hence increases linearly the skin friction and mass flow rate. Further, the velocity and temperature have the same behavior for different values of porous parameter when the temperature difference and the potential difference are in the same or in the opposite directions.

Keywords: Permeability, Oberbeck electro-convection, Poorly conducting fluid, Electric field, Perturbation technique, Skin friction.

INTRODUCTION

We note that in biomedical and bioengineering applications like cartilages in synovial joints (SJ) and endothelium in coronary arteries diseases (CA) involve porous layer saturated with poorly conducting fluid. At present artificial cartilages, and other organs are manufactured using metals. These organs manufactured by metals will have either rough or smooth surfaces and both of them are very dangerous due to a force resulting from these stresses. This force drives erythrocytes (i.e. RBC) in an artery to a particular region. The accumulation of RBCs in that region will be punctured resulting in the release of hemoglobin's. This leads to a disease called" Haemolysis". The objective of this paper is to propose a mechanism of overcoming this side effect by incorporating the porosity of the organs and using an electric field, assuming the body fluid in these organs as poorly conducing fluid saturated porous media. We note that (See Turnbull 1968, 1969) fluids of very low electrical conductivity like Nickle-Titanium

Rudraiah & Shashikala, Vol. 12, No. I, June, 2016, pp 1-12.

$(N_i - T_i)$, Aluminum-Nickle $(Al - N_i)$ alloys, and so on in the presence of electric field, known as electro hydrodynamics (EHD), permit EHD boundary layer flow separation (See Rudraiah *et. al.* 2003, 2006, 2007). Considerable interest has been evinced in the design of products and their use in modern technologies such as communication and information technology, transportation, production engineering, environmental and nuclear sciences, aerospace and defense, microelectronics, biology and so on. Each of these sectors needs material which minimizes the weight and vibrations and maximizes the efficiency. It is believed that such materials are smart materials of nanostructure. Nanoscience is the study and manufacture of structures and devices with dimensions about the size of few atoms or molecules. New materials like alloys having the functions of sensing and actuation properties are called smart materials. Usually sensing component of a smart structure is designed according to the nature of the event to be sensed. For example, thermal, mechanical or chemical as well as according to nature of output required such as thermal, electrical or mechanical. The sensors are used to duplicate the action of conventional strain gauges. Like sensing, the actuating component of smart material is also designed according to the nature of required actuation either thermal, mechanical or chemical as well as according to the nature of driving energy such as thermal, electrical and chemical. At present, as stated earlier, such materials are manufactured using piezoelectric materials. These piezoelectric materials are known to be ideal for ultrasonic applications due to their high frequency response. However, they may not be of much use for biomedical and bioengineering applications because they involve poorly electrically conducting fluids. Further, for high specific strength the piezoelectric materials exhibit anisotropy and in homogeneity leading to mathematical complications. These complications can be overcome by using the new smart materials made up of poorly conducting alloys proposed in this paper as an alternate to piezoelectric smart materials. The important process in the manufacture of this new smart material of nanostructure is the solidification of poorly conducting alloys like Nickel-Titanium (Ni-Ti), Aluminum-Nickel (Al-Ni) alloys and so on by cooling from below and heating from above. In these poorly conducting alloys, the electrical conductivity, σ, is a function of temperature which increases with an increase in temperature. The physical process involved in this solidification process is as follows. The variation of electrical conductivity with temperature releases free charges leading to distribution of charge density, ρ_e, resulting in induced electric field known as thermal electric field. In addition, there may be an applied electric field due to embedded electrodes at the boundaries. The total electric field, $\vec{E}$, namely the sum of induced and applied electric fields, produces not only the current, $\vec{J}$, which acts as a sensor and also an electric force, $\rho_e \vec{E}$, which acts as actuator. These two properties, sensing and actuating, are required a material to be a smart material. This electric force like buoyancy force produces a convective instability in a poorly conducting fluid while cooling from below and heating from above in the presence of electric field known as electro-convection (EC). A considerable amount of research has been devoted to the control of flow separation in ordinary or electrically conducting fluids (Rajgopal *et. al.* 1996) and in EHD because it is considered as an undesirable feature, but much attention has not been given to flow separation in EHD considering poorly conducting fluid saturated porous layer. This is considered in this paper. We know that ordinary techniques like suction or injection, blowing and wall movements are used for the control of separation, where as in EHD through porous layer considered in this paper an electric field is used to control flow separation. There has been a considerable practical interest in the study of convection in a vertical channel in the presence of electric field in a porous

Kathmandu University
Journal of Science, Engineering and Technology

Rudraiah & Shashikala, Vol. 12, No. I, June, 2016, pp 1-12.

medium. However, convection in a poorly conducting fluid saturated porous medium in the presence of an applied electric with porous medium considering the dissipations has not been given much attention in spite of their applications. The study of it is the main objective of this paper.

1. MATHEMATICAL FORMULATION:

The physical configuration considered in this problem is shown in fig 1. It consists of an infinite vertical porous channel bounded on both sides by the rigid isothermal plates embedded with electrodes located at $y = \pm b$ with x-axis in the axial direction and y-axis perpendicular to the plates. In addition to EHD and Oberbeck-Boussinesq approximations, we assume the porous layer is sparsely packed; the flow is fully developed and unidirectional in the x-direction, so that the velocity and temperature will be function of y only. The EHD assumptions enabled us to use the creeping flow approximations. The assumptions of Stokes and lubrication approximation make the above stated basic equations reduce to, conservation of mass

$$\nabla.\vec{q} = 0, \ \rho = \rho_0\left[1-\beta_T\left(T-T_0\right)\right] \qquad (2.1 \text{ a, b})$$

Since the porous layer is sparsely packed the conservation of momentum is the modified Darcy-Brinkman equations, modified in the sense of addition of electric force $\rho_e\vec{E}$ in the momentum equation and obtain

$$\bar{\nu}\frac{d^2u}{dy^2} - g\beta\Delta T - \frac{\nu}{k}u + \frac{\rho_e\vec{E}_x}{\rho_0} = 0 \qquad (2.2)$$

The energy equation with the addition of Ohmic, Darcy and viscous dissipations.

$$\frac{d^2T}{dy^2} + \frac{\bar{\mu}}{K}\left(\frac{du}{dy}\right)^2 + \frac{\sigma\left(E_x{}^2 + E_y{}^2\right)}{K} - \frac{\mu}{Kk}u^2 = 0 \qquad (2.3)$$

together with the conservation of charges

$$\nabla.\left(\sigma\vec{E}\right) = 0 \qquad (2.4)$$

and the Maxwell equations for a poorly conducting fluid

$$\nabla.\vec{E} = \frac{\rho_e}{\varepsilon_0}, \quad \vec{E} = -\nabla\phi, \quad \vec{J} = \sigma\vec{E}, \ \sigma = \sigma_0\left[1+\alpha_b\left(T-T_0\right)\right] \qquad (2.5 \text{ a, b, c, d})$$

Kathmandu University
Journal of Science, Engineering and Technology

Rudraiah & Shashikala, Vol. 12, No. I, June, 2016, pp 1-12.

2. METHOD OF SOLUTION, VELOCITY AND TEMPERATURE DISTRIBUTION:

Under these approximations, (2.2) to (2.5), after making them dimensionless using the scales

$$u^* = \frac{u}{g\beta b^2 (T_1 - T_0)/\nu},\ \theta = \frac{T - T_0}{\Delta T}, \rho_e^* = \frac{\rho_e}{\varepsilon_0 V/b^2}, E^* = \frac{E}{V/b},\ x^* = \frac{x}{b}, y^* = \frac{y}{b}, \sigma^* = \frac{\sigma}{\sigma_0} \qquad (3.1)$$

take the form

$$\frac{d^2u}{dy^2} - \delta^2 u + \frac{\theta}{\lambda} + \frac{W_e \rho_e \vec{E}_x}{\lambda} = 0 \qquad (3.2)$$

$$\frac{d^2\theta}{dy^2} + N\lambda\left(\frac{du}{dy}\right)^2 + N\sigma_p{}^2 u^2 + T_e\sigma\left(E_x{}^2 + E_y{}^2\right) = 0 \qquad (3.3)$$

$$\sigma\left(\nabla^2\phi\right) + \nabla\phi.\nabla\sigma = 0 \qquad (3.4)$$

$$\sigma = 1 + \alpha\theta, \alpha = \alpha_b \Delta T, \qquad (3.5)$$

where $W_e = \varepsilon_0 V^2/\rho_0 g\beta\Delta T b^3$ is the electric number, $N = \rho_0 g^2\beta^2(T_1 - T_0)b^4/K\nu$ the buoyancy parameter, $T_e = \sigma_0 V^2/K\Delta T$ the thermal electric number. $\delta^2 = \sigma_p{}^2/\lambda$, $\sigma_p{}^2 = b^2/k$ the porous parameter, $\lambda = \bar{\nu}/\nu$ is the ratio of effective viscosity to viscosity of fluid. The required boundary conditions, shown in fig 1, after making them dimensionless, are

$$u = 0\ at\ y = \pm 1, \theta = 1\ at\ y = 1, \theta = -1\ at\ y = -1 \qquad (3.6\ a, b, c)$$

The solutions of these equations are determined in the subsequent sections both analytically and numerically, using these boundary conditions.

3. SOLUTION FOR ϕ:

The solution for ϕ, according to (3.4) depends on σ which in turn depends on the temperature θ as in (3.5). In a poorly conducting fluid (i.e., σ<<1), to find σ ,we assume the dissipations in (3.3) are negligible and hence σ will depend on the conduction temperature, θ_B ,satisfying

$$\frac{d^2\theta_B}{dy^2} = 0 \qquad (4.1)$$

The solution of this satisfying the boundary conditions

$$\theta_B = 1 \quad at \quad y = 1\ and\ \theta_B = -1\ at \quad y = -1 \qquad (4.2) \quad \text{is} \quad \theta_B = y \qquad (4.3)$$

Kathmandu University
Journal of Science, Engineering and Technology

Rudraiah & Shashikala, Vol. 12, No. I, June, 2016, pp 1-12.

Then (3.5) becomes $\sigma = 1 + \alpha y \approx e^{\alpha y} \ (\because \alpha << 1)$ (4.4)

Eqn (3.4) using (4.4) becomes $\frac{\partial^2 \phi}{\partial x^2} + \frac{\partial^2 \phi}{\partial y^2} + \alpha \frac{\partial \phi}{\partial y} = 0$ (4.5)

To find the solution of (4.5), we consider the following two cases:

Case 1: The Potential Difference Applied Opposite to the Temperature Difference

In this case the boundary conditions as shown in fig.1, making them dimensionless, are

$$\phi = x \quad at \quad y = -1 \quad and \quad \phi = x - x_0 \quad at \quad y = 1 \tag{4.6}$$

The solution of (4.5), satisfying (4.6), is $\phi = x - \frac{x_0}{2Sinh\alpha}\left(e^{\alpha} - e^{-\alpha y}\right)$ (4.7)

From (2.5, a, b, c, d), after making dimensionless using the quantities defined earlier and using (4.7), we get $\rho_e = \nabla.\vec{E} = -\nabla^2\phi = -\frac{\alpha^2 x_0 e^{-\alpha y}}{2Sinh\alpha}$, $E_x = -1, E_y = \frac{\alpha x_0 e^{-\alpha y}}{2Sinh\alpha}$ (4.8)

Also $\rho_e E_x = \frac{\alpha^2 x_0 e^{-\alpha y}}{2Sinh\alpha}, E^2{}_x + E^2{}_y = 1 + \frac{x_0{}^2 \alpha^2 e^{-2\alpha y}}{4Sinh^2\alpha}$ (4.9)

Case 2: The Potential Difference Applied in the Same Direction of Temperature Difference

In this case the boundary conditions on ϕ, in dimensionless form, are opposite to those specified in (4.6) and they are $\phi = x \quad at \quad y = 1 \quad and \quad \phi = x - x_0 \quad at \quad y = -1$ (4.10)

In this case the solution of (4.5), satisfying (4.10), is $\phi = x + \frac{x_0}{2Sinh\alpha}\left(e^{-\alpha} - e^{-\alpha y}\right)$ (4.11)

In this case ρ_e, E_y and $\rho_e E_x$ are opposite to those obtained in case 1, whereas E_x and $E_x{}^2 + E_y{}^2$ remain the same as in case 1. Equations (3.2) and (3.3) are coupled nonlinear equations because of dissipation terms, which are solved both analytically and numerically in the next section.

4. ANALYTICAL SOLUTIONS:

Analytical solutions for velocity and temperature are obtained using a regular perturbation technique, with the buoyancy parameter N as the perturbation parameter, which is very small. We look for the solutions of (3.2) and (3.3) in the form

Kathmandu University
Journal of Science, Engineering and Technology

Rudraiah & Shashikala, Vol. 12, No. I, June, 2016, pp 1-12.

$$u = u_{0+}Nu_1 + N^2u_2 + \cdots, \theta = \theta_0 + N\theta_1 + N^2\theta_2 + \cdots, \qquad (5.1\ a, b)$$

Here the subscript 0 refers to the solutions for the case in which N=0, which represents physically the solutions in the absence of viscous dissipation and $u_1, u_2 ....., \theta_1, \theta_2 ....., ,$ are the perturbation quantities which are assumed to be small compared to u_0 *and* θ_0. Equations (3.2) and (3.3), using (4.11) and (5.1a, b) and equating the coefficients of the like powers of N to zero, we get the following set of equations:

Zeroth order equations: For case 1: $$\frac{d^2u_0}{dy^2} - \delta^2 u_0 + \frac{\theta_0}{\lambda} + W_1 e^{-\alpha y} = 0 \qquad (5.2)$$

For case 2: $$\frac{d^2u_0}{dy^2} - \delta^2 u_0 + \frac{\theta_0}{\lambda} + W_2 e^{-\alpha y} = 0 \qquad (5.3)$$

$$\frac{d^2\theta_0}{dy^2} + T_e e^{\alpha y} + W_3 e^{-\alpha y} = 0 \qquad (5.4)$$

First order equations:

$$\frac{d^2u_1}{dy^2} - \delta^2 u_1 + \frac{\theta_1}{\lambda} = 0 \qquad (5.5)$$

$$\frac{d^2\theta_1}{dy^2} + \lambda\left(\frac{du_0}{dy}\right)^2 + \sigma_p{}^2 u_0{}^2 = 0 \qquad (5.6)$$

where $W_1 = \frac{W_e\alpha^2 x_0}{2\lambda Sinh\alpha}$ for case1, $W_2 = -\frac{W_e\alpha^2 x_0}{2\lambda Sinh\alpha}$ and $W_3 = \frac{T_e\alpha^2 x_0{}^2}{4Sinh^2\alpha}$ are constants.

These equations are solved, using the boundary conditions, in dimensionless form,

$$\begin{aligned} &\theta_0 = 1 at\ y = 1, \theta_0 = -1 at\ y = -1 \\ &u_0 = u_1 = \theta_1 = 0 \quad at \quad y = \pm 1 \end{aligned} \qquad (5.7)$$

Solutions of (5.2) to (5.6), satisfying the conditions (5.7), are

$$\theta_0 = y\alpha^2 + T_e(Cosh\alpha - e^{\alpha y} + ySinh\alpha) + W_2(Cosh\alpha - e^{-\alpha y} - ySinh\alpha)/\alpha^2 \qquad (5.8)$$

Kathmandu University
Journal of Science, Engineering and Technology

Rudraiah & Shashikala, Vol. 12, No. I, June, 2016, pp 1-12.

$$u_0 = \frac{T_e}{\alpha^2\left(\alpha^2-\delta^2\right)\lambda}\left[\frac{e^{\alpha y}Sinh2\delta - 2Sinh\delta Cosh\alpha Cosh\delta y - 2Sinh\alpha Cosh\delta Sinh\delta y}{Sinh2\delta}\right]+$$
$$\frac{a_1}{\left(\alpha^2-\delta^2\right)}\left[\frac{e^{-\alpha y}Sinh2\delta + 2Sinh\alpha Cosh\delta Sinh\delta y - 2Sinh\delta Cosh\alpha Cosh\delta y}{Sinh2\delta}\right]+ \quad (5.9)$$
$$\frac{c_2}{\delta^2\lambda}\left[1-\frac{Cosh\delta y}{Cosh\delta}\right]+c_1\left[y-\frac{Sinh\delta y}{Sinh\delta}\right]$$

$$\theta_1 = a_{33}Cosh2\delta y + \frac{a_4 Sinh2\delta y}{4\delta^2} + a_{25}e^{\alpha y}Cosh\delta y + a_{26}e^{\alpha y}Sinh\delta y + a_{27}e^{-\alpha y}Cosh\delta y + a_{28}e^{-\alpha y}Sinh\delta y$$
$$+a_{29}Cosh\delta y + a_{30}Sinh\delta y - \frac{2c_4c_1{\sigma_p}^2 ySinh\delta y}{\delta^4\lambda} - \frac{2c_3c_1{\sigma_p}^2 yCosh\delta y}{\delta^4\lambda} + \frac{a_{11}}{4\alpha^2}e^{2\alpha y} + \frac{a_{12}}{4\alpha^2}e^{-2\alpha y} \quad (5.10)$$
$$-\frac{2T_e c_1{\sigma_p}^2}{\delta^2\lambda^2\alpha^4(\alpha^2-\delta^2)}ye^{\alpha y} - \frac{2a_1c_1{\sigma_p}^2}{\delta^2\lambda\alpha^2(\alpha^2-\delta^2)}ye^{-\alpha y} + a_{31}e^{\alpha y} + a_{32}e^{-\alpha y} - \frac{c_1c_2{\sigma_p}^2}{3\delta^4\lambda^2}y^3$$
$$-\frac{c_1^2{\sigma_p}^2}{12\delta^4\lambda^2}y^4 + \frac{a_{24}}{2}y^2 + \frac{(p_2-p_1)}{2}y + \frac{(-p_2-p_1)}{2}$$

$$u_1 = \frac{(p_4-p_3)}{2}\frac{Sinh\delta y}{Sinh\delta} - \frac{(p_3+p_4)}{2}\frac{Cosh\delta y}{Cosh\delta} - \frac{a_{33}}{3\delta^2\lambda}Cosh2\delta y - \frac{a_4}{12\delta^4\lambda}Sinh2\delta y$$
$$+\frac{c_1c_4{\sigma_p}^2}{2\delta^5\lambda^2}y^2Cosh\delta y + \frac{c_1c_3{\sigma_p}^2}{2\delta^5\lambda^2}y^2Sinh\delta y + a_{34}yCosh\delta y + a_{35}ySinh\delta y$$
$$-\frac{a_{11}}{4\lambda\alpha^2(4\alpha^2-\delta^2)}e^{2\alpha y} - \frac{a_{12}}{4\lambda\alpha^2(4\alpha^2-\delta^2)}e^{-2\alpha y} + a_{36}e^{(\alpha+\delta)y} + a_{37}e^{(\alpha-\delta)y} + a_{38}e^{-(\alpha-\delta)y} \quad (5.11)$$
$$+a_{37}e^{-(\alpha+\delta)y} + \frac{2T_e c_1{\sigma_p}^2}{\delta^2\lambda^3\alpha^4(\alpha^2-\delta^2)^2}ye^{\alpha y} + \frac{2a_1c_1{\sigma_p}^2}{\delta^2\lambda^2\alpha^2(\alpha^2-\delta^2)^2}ye^{-\alpha y} + a_{40}e^{\alpha y}$$
$$+a_{41}e^{-\alpha y} - \frac{c_1^2{\sigma_p}^2}{12\delta^6\lambda^3}y^4 - \frac{c_1c_2{\sigma_p}^2}{3\delta^6\lambda^3}y^3 + a_{42}y^2 + a_{43}y + a_{44}$$

The velocity (u) and temperature (θ), can be obtained respectively using (5.1a, b) and (5.2) to (.5.6). We note that a_1 , given in the appendix, involve W_1 for case 1 and W_2 for case2. These u and θ are computed for the cases1 and 2 and the results are depicted in figs (4.2) to (4.6).

5. NUMERICAL SOLUTIONS:

We obtain numerical solution, using a finite difference technique. The velocity and energy equations are solved using the central difference method. The use of central difference scheme replaces the derivatives with corresponding central difference approximations leading to set of linear algebraic equations. The solution of reduced algebraic equations is obtained by the method of Successive Over Relaxation (SOR). The relaxation parameter ω is fixed by comparing the numerical results with those obtained by analytical method. The convergence criterion is based on the step size and the previous iterations for the iterative difference to the order10^{-6}.

Kathmandu University
Journal of Science, Engineering and Technology

Rudraiah & Shashikala, Vol. 12, No. I, June, 2016, pp 1-12.

The finite difference equations equivalent to (3.2) and (3.3) with 21 mesh point with the step size 0.1 are

$$\frac{u_{j-1}-2u_j+u_{j+1}}{(\Delta y)^2}-\delta^2 u_j+\frac{\theta_j}{\lambda}+W_1 e^{-\alpha y_j}=0$$

Solving for u_j, $u_j=\frac{1}{\left(2+\delta^2(\Delta y)^2\right)}\left[u_{j-1}+u_{j+1}+\frac{\theta_j(\Delta y^2)}{\lambda}+W_1 e^{-\alpha y_j}(\Delta y)^2\right]$ (6.1)

$$\frac{\theta_{j-1}-2\theta_j+\theta_{j+1}}{(\Delta y)^2}+N\lambda\left(\frac{u_{j+1}-u_{j-1}}{2\Delta y}\right)^2+N\sigma_p{}^2 u_j{}^2+T_e e^{\alpha y_j}+W_2 e^{-\alpha y_j}=0$$

Solving for θ_j

$$\theta_j=\frac{1}{2}\left[\begin{array}{l}\theta_{j-1}+\theta_{j+1}+\frac{N\lambda}{4}\left(u_{j+1}-u_{j-1}\right)^2+N\sigma_p{}^2(\Delta y)^2 u_j{}^2+T_e(\Delta y)^2 e^{\alpha y_j}\\ +W_2(\Delta y)^2 e^{-\alpha y_j}\end{array}\right] \quad (6.2)$$

Applying SOR, we obtain from (4.6.1) and (4.6.2),

$$U(J)=\frac{\omega}{\left(2+\delta^2(\Delta y)^2\right)}\left[U(J-1)+U(J+1)+W_1(\Delta y)^2 Exp(-\alpha y_j)+\frac{\theta I(J)(\Delta y)^2}{\lambda}\right]+(1-\omega)UI(J) \quad (6.3)$$

$$\theta(J)=\frac{\omega}{2}\left[\begin{array}{l}\theta(J-1)+\theta(J+1)+\frac{N\lambda}{4}\left(UI(J+1)-U(J-1)\right)^2+N\sigma_p{}^2(\Delta y)^2 U(J)*U(J)\\ +T_e(\Delta y)^2 Exp(\alpha y_j)+W_2*(\Delta y)^2 Exp(-\alpha y_j)\end{array}\right] \quad (6.4)$$
$$+(1-\omega)\theta I(J)$$

In (6.3) and (6.4), ω is the relaxation parameter. The value of ω is fixed at 1.645 after checking the closeness with analytical solutions. These solutions (6.1) and (6.2) are computed for different values of the parameters. We find the skin friction, rate of heat transfer and mass flow rate and the results are depicted in figs (4.4) to (4.6).

Kathmandu University
Journal of Science, Engineering and Technology

Rudraiah & Shashikala, Vol. 12, No. I, June, 2016, pp 1-12.

RESULTS AND DISCUSSIONS

The effects of electric field and porous parameter on the velocity (u), temperature (θ), Skin friction, Rate of heat transfer (Nu) are obtained analytically, using a regular perturbation technique valid for small values of buoyancy parameter N. The velocity given by (5.1a), is computed for different values of the electric number W_e, Porous parameter σ_p and the ratio of viscosities λ and the results are depicted in figs (4.2 a, b, c), when the potential and temperature differences are either in the same direction or opposing each other. From these figures we conclude the following:

1. The velocity profile is still parabolic even in electro hydrodynamics through porous media as in hydrodynamics with the exception that it increases with an increase in electric number W_e. This increase is more when the temperature difference opposes the potential difference compared to that when the temperature difference is in the same direction of potential difference.

2. An increase in the porous parameter σ_p decreases the velocity, as expected on physical grounds namely σ_p dampens the velocity.

3. An increase in the ratio of viscosities, λ, decreases the velocity, because of the resistance offered to the flow. From the above results we conclude that an electric field, porous parameter and the ratio of viscosities can be effectively used to control OBEC. Similarly, the temperature θ, given by (5.1b), is computed for different values of Te, We, σ_p and the results are depicted in fig (4.3) and tabulated in the above tables1 and 2 respectively. From this figure (4.3), we conclude that an increase in T_e also increases the temperature and the rate of increase is slightly greater when the temperature difference and the potential difference are in the same directions compared to those in the opposite directions. In particular, we note that for different values of We, the temperature profile depicts the nature of parabolic implying temperature tends to dominate conduction than convection. Physically this implies that the effect of W_e is to suppress convection. The skin friction is computed for different values of We and N, and the results are depicted in figs (4.4a, b). Fig (4.4a), revels that an increase in We increases the skin friction, whose increase is more in case 2 than that in case1.Fig (4.4b), revels that, an increase in N decreases the skin friction, as expected on physical grounds. But the rate of decrease is more in case2 compared to that in case1.In figs (4.5a) and (4.5b), the rate of heat transfer is depicted. Fig (4.5a) is a plot of the rate of heat transfer or local Nusselt number N_u verses We. It reveals that Nu decreases with an increase in We and tends to a constant value. But the rate of decrease is more in case2 compared to case1. Fig (4.5b), represents the rate of heat transfer Nu plotted verses σp and its effect is to increase Nu with an increase in σp. We note that this rate of increase is more in case2 compared to that in case1. Fig (4.6), represents the mass flow rate vs electric number for different values of N. Here we observe that the mass flow rate decreases with an increase in N. Finally, we conclude that with a proper choice of an external constraint of electric field, permeability and ratio of viscosities, it is possible to control OBEC, which is useful in the manufacture of novel materials like smart materials free from impurities.

Kathmandu University
Journal of Science, Engineering and Technology

Rudraiah & Shashikala, Vol. 12, No. I, June, 2016, pp 1-12.

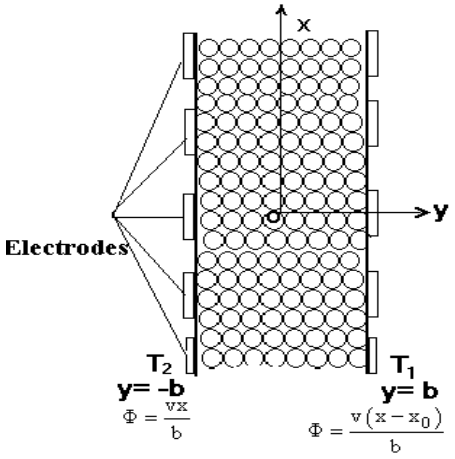

Fig4.1: Physical configuration

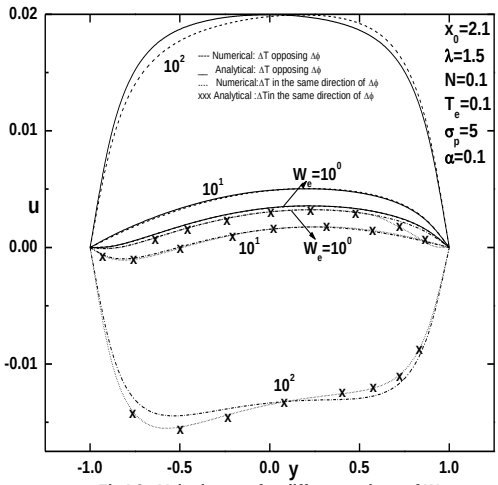

Fig4.2a:Velocity vs y for different values of W_e

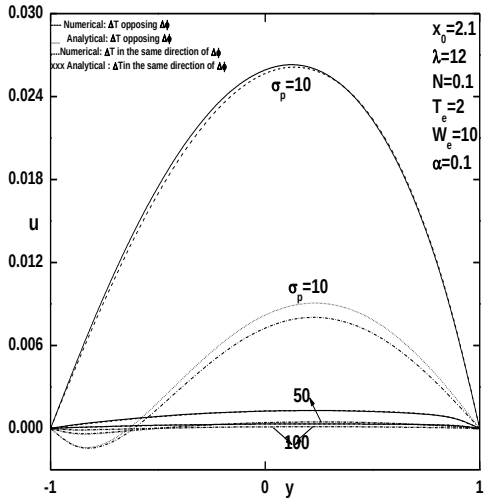

Fig4.2b:Velocity vs y for different values of σ_p

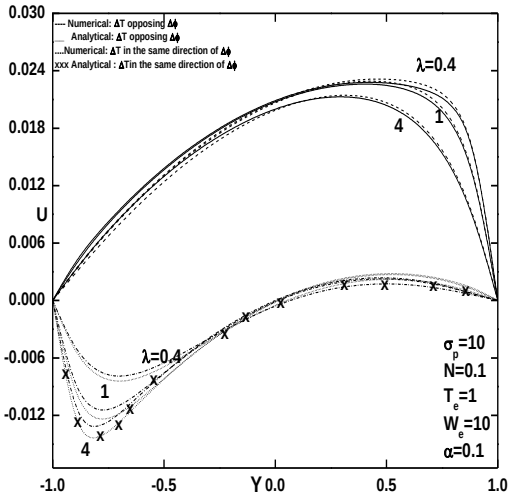

Fig4.2c:Velocity vs y for different values of λ

Kathmandu University
Journal of Science, Engineering and Technology

Rudraiah & Shashikala, Vol. 12, No. I, June, 2016, pp 1-12.

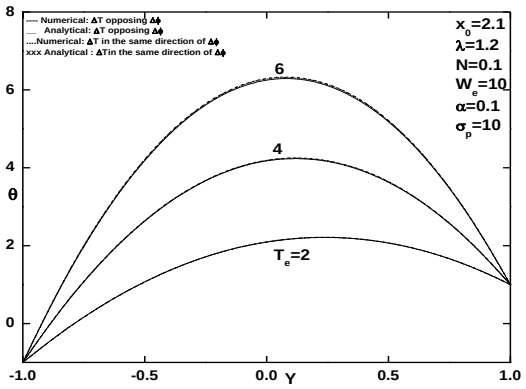

Fig4.3:Temperature vs y for different values of T_e

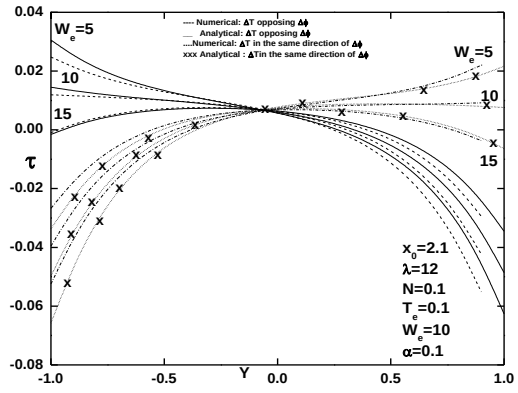

Fig4.4a:Skinfriction vs y for different values of W_e

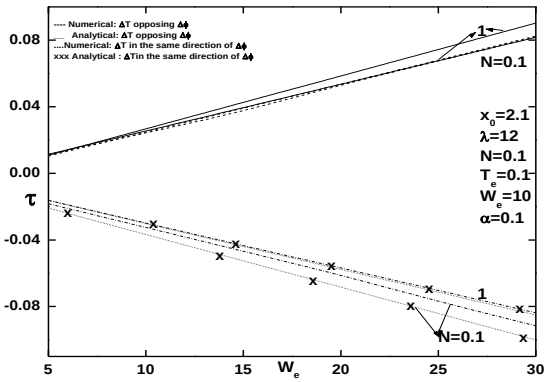

Fig4.4b:Skin friction vs W_e for different values of N

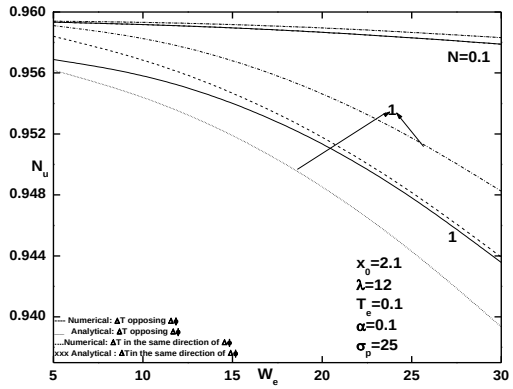

Fig4.5a:Heat transfer vs W_e for different values of N

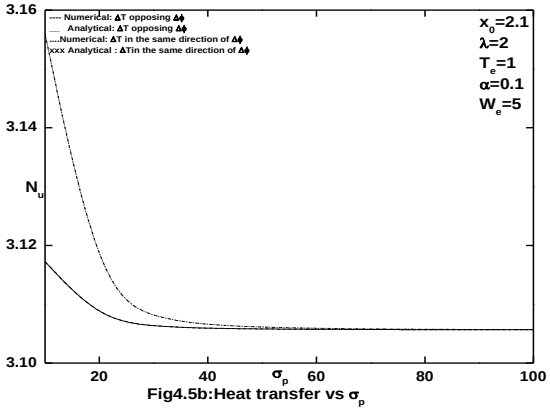

Fig4.5b:Heat transfer vs σ_p

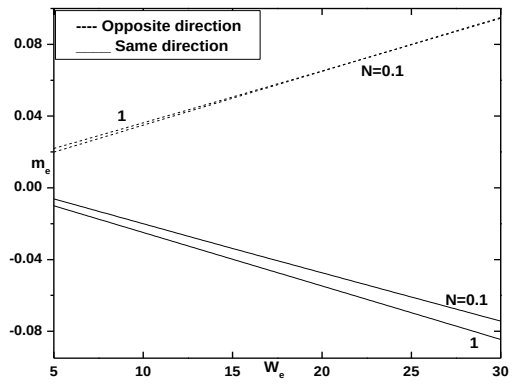

Fig4.6:Mass flow rate vs electric number for different values of N

Rudraiah & Shashikala, Vol. 12, No. I, June, 2016, pp 1-12.

ACKNOWLEDGMENTS

The work is supported by Technical education and Principal of GSKSJTI, K.R Circle, Bangalore-01.

REFERENCES

[1] Rudraiah N, Modeling of Nano and Smart Materials, *Book paradise*, India, 2003.

[2] Rudraiah N & Ng C O, A model for manufacture of nano-sized smart materials free from impurities, *Curr. Sci.,* (2004) 86(8): 1076 (review articles).

[3] Turnbull R J, Electro-convective instability with a stabilizing temperature gradient-I theory, *Phys. Fluids,* (1968) 11(12): 2588.

[4] Turnbull R J, Free convection from a heater vertical plate in a direct current electric field, *Phys. Fluids*, (1969) 12(11): 2255.

[6] Malkus W V R & Veronis G, Surface electro-convection, *Phys. Fluids,* (1961) 4(1): 13.

[7] Rudraiah N, Masuoka T & Nair P, Effect of combined Brinkman and electro boundary layer on the onset of Marangoni electro-convection in a poorly conducting fluid-saturated porous layer cooled form below in the presence of an electric field, *J. Porous Media*, (2007) 10(5).

[8] Rajgopal K R *et al.*, On the Oberbeck–Boussinesq approximation, *Mathematical Models and Methods in Applied Sciences,* (1996) 6(8): 1157–1167.

[9] Rudraiah N & Shashikala B S, Non-linear Oberbeck electro-convection in a poorly conducting fluid through a vertical channel in the presence of an electric field, *International Journal of Non-Linear Mechanics*, (2007) 42: 403-410.